CDF/ANAL/CDF/CDFR/9242
Draft 2.0
July 16, 2008

Using Drell-Yan to Probe the Underlying Event in Run 2 at CDF

Deepak Kar[1], Rick Field[2]

University of Florida, Gainesville, FL
On Behalf of the CDF Collaboration

Abstract

We study the event topology in Drell-Yan lepton-pair production in proton-antiproton collisions at 1.96 TeV in Run 2 at CDF. We use the direction of the lepton-pair on an event by event basis to define three regions of $\eta - \phi$ space; toward, away and transverse. The transverse and toward regions are very sensitive to the underlying event. The data are corrected back to the particle level and are then compared with the PYTHIA tune AW. The properties of the underlying event are examined as a function of the lepton-pair transverse momentum. The data are also compared with a previous analysis on the behavior of the underlying event in high transverse momentum jet production. The goal is to improve our understanding and modeling of the high energy collider events.

[1]dkar@phys.ufl.edu
[2]rfield@phys.ufl.edu

1 Introduction

The goal of this analysis is to present measurements sensitive to the underlying event that are corrected back to the particle level so that they can be used to tune the QCD Monte Carlo models without requiring CDF detector simulation and to compare with a similar analysis done with the Tevatron jet data.

2 Introduction

The goal of this analysis is to present measurements sensitive to the underlying event that are corrected back to the particle level so that they can be used to tune the QCD Monte Carlo models without requiring CDF detector simulation and to compare with a similar analysis done with the Tevatron jet data.

2.1 Underlying Event in a Typical Collider Event

A typical 2-to-2 hard scattering event in a proton-antiproton collision at the hadron colliders as shown in the Fig. 1. The incoming fundamental particles are the quarks and gluons inside the hadrons and the strong force is the dominant interaction.

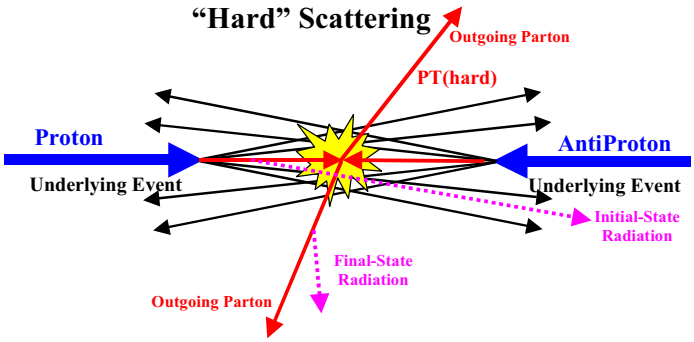

Figure 1: Components of a 2-2 Hard Scattering

Except the two hard scattered outgoing partons - the landscape is dominated by initial and final state radiation (caused by bremsstrahlung and gluon emission), resonance decays, multiple parton interaction (additional 2-to-2 scattering within the same event), hadronization, beam beam remnants (particles that come from the breakup of the proton and antiproton) and so on.

We define the 'underlying event' as everything except the two outgoing hard scattered 'jets' and consists of the 'beam-beam remnants' plus initial and final-state radiation[1]. However experimentally, it is impossible to seperate out the two components. The 'hard scattering' component consists of the outgoing two 'jets' plus initial and final-state radiation. The 'beam-beam remnants' are what is left over after a parton is knocked out of each of the initial two beam hadrons as in Fig. 3. It is the reason hadron-hadron collisions are more 'messy' than electron-positron annihilations and no one really knows how it should be modeled. Also, it is possible that multiple parton scattering, as in Fig. 2 contributes to the 'underlying event'. In addition to the hard 2-to-2 parton-parton scattering and the 'beam-beam remnants', sometimes there is a second 'semi-hard' 2-to-2 parton-parton scattering that contributes particles to the "underlying event" as in Fig. 2.

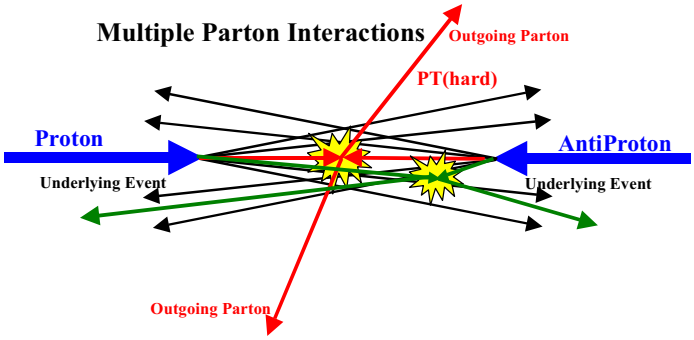

Figure 2: Multiple Parton Interactions

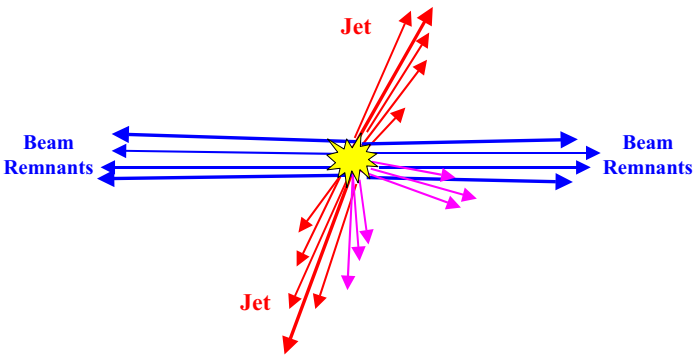

Figure 3: Beam Beam Remnants

2.2 Transverse, Toward and Away Regions

We would now define and look at the different regions at a collider event. The angle $\Delta\phi = \phi - \phi_{leadingjet}$ is the relative azimuthal angle between charged particles and the direction of hard scattered leading jet. Later we would be looking at lepton pair production from Z boson, $\Delta\phi$ would then be determined relative to the direction of Z boson. Now we can split the central region, defined between $|\eta| < 1$ as in Fig. 4.

- $|\Delta\phi| < 60^\circ$ as toward region.
- $60^\circ < |\Delta\phi| < 120^\circ$ as Transverse region. And,
- $|\Delta\phi| > 120^\circ$ as away region.

For hard scattered jets, where the relative azimuthal angle is with respect to the leading jet direction, the transverse regions are the most sensitive to underlying events, since they are perpendicular to the plane of 2-to-2 hard scattering. For them we have outgoing jets in transverse regions, almost impossible to separate them out from the background.

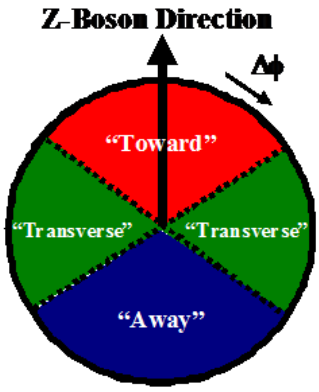

Figure 4: Different Regions in $\eta - \phi$ space

2.3 The Drell Yan Process

Quarks and antiquarks from the incoming hadron beams annihilate to produce a virtual photon or Z^0, which decays to a lepton pair (e^+e^- or $\mu^+\mu^-$).

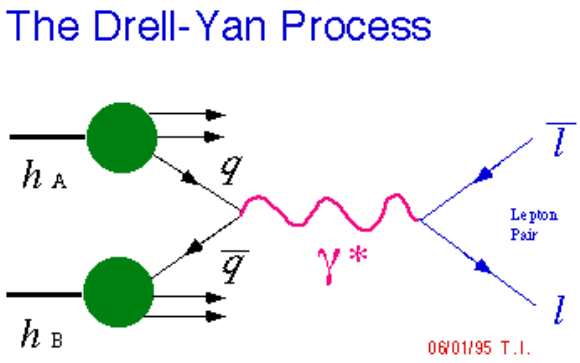

Figure 5: Drell Yan Process

Let us compare the underlying events in a hard scattering as in Fig. 1 with underlying events in Drell Yan process.

By looking at the diagram we can see that essentially everything other than the final lepton-antilepton pair is the underlying event for the low P_T case. For Drell-Yan it is easy

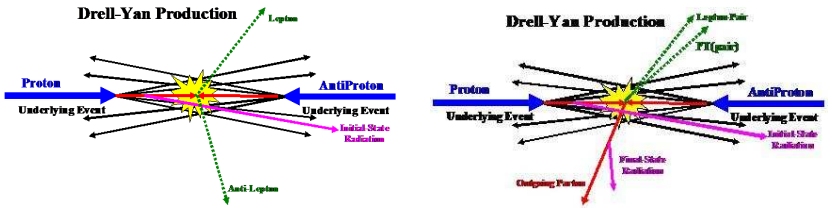

Figure 6: Underlying event in Drell-Yan. Left: Low P_T, Right: High P_T

to identify and remove leptons (since they are the colorless components) from the transverse and toward regions to study the underlying event.

Single Z Bosons are produced with large P_T via the ordinary QCD sub processes, generating additional gluons via bremsstrahlung resulting in multi-parton final states fragmenting into hadrons and forming away-side jets. The transverse region is perpendicular to the hard scattering and once we remove the lepton pair from the toward region we are left with only underlying event in these two regions.

So we can see not only Drell Yan events are a clean probe of the underlying event but also we can study the underlying event as a function of lepton pair transverse momentum or invariant mass. Comparing them with high P_T jet production would help us to learn more about underlying event in general. And at the same time we would be able to look at Z boson P_T distribution, which would an extra way to constrain our underlying event model.

3 Data Selection and Lepton Identification

3.1 Data Selection

We analyze the High P_T Electron and Muon Data and corresponding PYTHIA tune AW (tuned to fit the underlying event and the Run 1 Z-boson P_T distribution) stntuples, as shown in Table 1. We analyzed data till Run Period 17, corresponding to the luminosity of approximately 2.7 fb^{-1}. Data and detector level Monte Carlo passes through the same selection critea.

Table 1: Datasets Used

Lepton	Monte Carlo	DATA (Trigger)
Electron	ze0s, ze1s (Drell- Yan Z/gamma* Sample, $Z \rightarrow ee$)	bhel (high-P_T Central electrons)
Muon	ze0s, ze1s (Drell- Yan Z/gamma* Sample, $Z \rightarrow \mu\mu$)	bhmu (high-P_T CMUP and CMX muons)

3.2 Event Selection

Events are required to be on the goodrun list, version 23. We pick only those events having one and only one quality 12 vertex within $|Z_0| < 60$ cm. It measures the distance of the $p\overline{p}$ collision event vertex from the center of the detector in z direction. To ensure that track for each particle is well extrapolated to the calorimeter and drift chamber, we need that restriction.

3.3 Electron Selection

The electron selections are based on the high P_T electron selection criteria as mentioned in CDF note 7950 [4], which is also on the CDF Joint Physics webpage. We look at Central electrons, with tight and loose cuts described in table[2], and check that they are not conversion electrons. The tight and loose cuts are similar till the last four variables in the table, i.e. loose electrons are tight electrons without the L_{Shr}, E/p, signed CES ΔX, CES ΔZ and CES Strip χ^2 cuts.

Table 2: Electron Selection

Variable	Loose	Tight
Region	CEM	CEM
Fiducial	1	1
E_T	$\geq$ 20 GeV	$\geq$ 20 GeV
Track Z_0	$\leq$ 60 cm	$\leq$ 60 cm
Track p_T	$\geq$ 10 GeV/c	$\geq$ 10 GeV/c
COT Axial	3 Axial SLs with 5 hits/SL	3 Axial SLs with 5 hits/SL
COT Stereo	2 Stereo SLs with 5 hits/SL	2 Stereo SLs with 5 hits/SL
Isolation(R=0.4)/E_T	≤ 0.1	≤ 0.1
(with leakage correction)		
E_{Had}/E_{EM} (3 towers)	$\leq (0.055 + (0.00045 \times E))$	$\leq (0.055 + (0.00045 \times E))$
L_{Shr} (3 towers, track)		≤ 0.2
E/p		$\leq$ 2.0(unless $P_T \geq$ 50 Gev/c)
CES ΔZ		$\leq$ 3.0 cm
Signed CES ΔX		$-3.0 \leq q \times \Delta X \leq 1.5$
CES Strip χ^2(Scaled with E)		$\leq$ 10.0

3.4 Muon Selection

The muon selections are based on the high P_T muon selection criteria as mentioned in CDF note 8262 [5], which is also on the CDF Joint Physics webpage. We look at the CMUP and CMX muons, with 'fiducial cuts' in addition to the standard cuts, as in table[3]. The only extra cut we make is on χ^2/DoF - which helps to eliminate cosmic muons. Apart from that, to get rid of cosmic muons, we also use a Time of Flight (TOF) cosmic filter, which would be described in more details in the next section.

3.5 Lepton Pair Formation

The lepton pairs are formed by oppositely charged leptons, with the requirement that Z_0 of the two leptons must pass $|z_0^1 - z_0^2| < 4$ cm, to ensure that both leptons came from the same primary collision. For electrons, we form pairs with at least one tight electron, as defined earlier. For Muons, there is no such distinction. Additionally for rejecting cosmic muons, we implement TOF (Time of Flight) timing cuts from CDF note 6073[6]. If both muons have TOF timing, we require the difference of the TOF times between the upper and the lower muon to be less than 5 ns. Timing is a good way to distinguish if two muons came from the interaction point, or one single muon from a cosmic ray appear to be as two muons. The time difference between the muons recorded in the upper and lower half of the detector, as measured by the Time of Flight detector is given as,

$$\begin{aligned} \Delta_T &= T_{upper} - T_{lower} \\ &= (L_1 + L_2)/c \\ &\approx 2L_1/c \approx 2L_2/c \end{aligned}$$

Table 3: Muon Selection

Variable	Muon
For All Muon Types	
Region	CMUP and CMX
P_T	$\geq$ 20 GeV/c
E_{EM}	$\leq$ 2 GeV + Max(0,(0.0115 $\times$(p-100))
E_{Had}	$\leq$ 6 GeV + Max(0,(0.028 $\times$(p-100))
Isolation (Total ET in R=0.4 around muon)/P_T	$\leq$ 0.1
COT Axial	3 Axial SLs with 5 hits/SL
COT Stereo	2 Stereo SLs with 5 hits/SL
Track $\lvert Z_0 \rvert$	$\leq$ 60 cm
Track $\lvert d_0 \rvert$ (Beam Corrected)	$\leq$ 0.2 cm
Additionally for CMUP Muons	
$\lvert \Delta X_{CMU} \rvert$	$\leq$ 7 cm
$\lvert \Delta X_{CMP} \rvert$	$\leq$ 5 cm
$X - FID_{CMU}$	$\leq$ 0 cm
$X - FID_{CMP}$	$\leq$ 0 cm
$Z - FID_{CMU}$	≤ -3 cm
$Z - FID_{CMP}$	$\leq$ 0 cm
Additionally for CMX Muons	
$\lvert \Delta X_{CMX} \rvert$	$<$ 6 cm
Run Number $>$ 150144	
$X - FID_{CMX}$	$<$ 0 cm
$Z - FID_{CMX}$	< -3 cm
To Remove Cosmic Muons	
$\lvert \Delta z \rvert$	$\leq$ 3 cm
Track Fit χ^2/DoF	$\leq$ 2.3

Where L_1 and L_2 are the distances traveled by the cosmic ray in the upper and the lower half of the detector. For two muons originating at the center of the detector,

$$\Delta_T = T_{upper} - T_{lower}$$
$$= (L_1 - L_2)/c$$
$$\approx 0$$

So ideally the muons not coming from the cosmic rays would have very little time difference, and this principle is used to eliminate cosmic ray muons.

The mass range of the lepton pair is divided into 3 regions for this analysis, as shown in Table 4. The 70 GeV/c^2 < invariant mass of the lepton pair < 110 GeV/c^2, termed the Z-region, is where we concentrate for now.

Table 4: Mass Ranges

Mass Region	Mass Range
Low	Less than 70 GeV/c^2
Z	70-110 GeV/c^2
High	Above 110 GeV/c^2

Approximately 65000 electron and muon pairs passed our selection criteria and are used in the analysis.

3.6 Charged Track Selection

Only charged tracks in the region 0.5 GeV/c < P_T < 150 GeV/c and $|\eta| < 1$, where efficiency is high are considered. The upper limit of P_{Tmax} cut is chosen to prevent miss-measured tracks with very high P_T from contributing to the observables.

The track selection criteria is given in Table 5.

Table 5: Charged Track Selection

Variable	Loose	Tight
Track Region	COT	COT
Track P_T Min	≥ 0.5 GeV/c	≥ 0.5 GeV/c
Track P_T Max	≤ 150 GeV/c	≤ 150 GeV/c
Track $\|\eta\|$	≤ 1	≤ 1
Track Z_0	< 60 cm	< 60 cm
Track $\|d_0\|$ (Beam Corrected)	≤ 1 cm	≤ 0.5 cm
Track $\|\Delta z\|$	≤ 3 cm	≤ 2 cm
COT Axial	2 Axial SLs with 10 hits/SL	2 Axial SLs with 10 hits/SL
COT Stereo	2 Stereo SLs with 10 hits/SL	2 Stereo SLs with 10 hits/SL
Track Fit χ^2/DoF	≤ 10	≤ 10

3.7 Observables

Some of the observables that are studied in this analysis are described in Table 6. Since we would be studying regions in $\eta - \phi$ space with different areas, as defined in Section 1.2 we will construct densities by dividing by the area. The mean charged particle $< P_T >$ is constructed on an event by event basis and then averaged over the events. For the average P_T and P_{TMax} we require that there is at least one charged particle present. The P_{Tsum} (hence the P_{Tsum} density) is taken to be zero if there are no charged particles present.

Table 6: Observables

Observable	Particle Level	Detector Level
Lepton P_T	P_T of the lepton pair	P_T of the lepton pair, formed by at least one tight lepton.
Lepton P_T Squared	P_T squared of the lepton pair	P_T squared of the lepton pair, formed by at least one tight lepton.
Charged Density	Number of charged particles per unit $\eta - \phi$	Number of 'good' charged tracks per unit $\eta - \phi$
$< P_T >$	Average P_T of charged particles	Average P_T of 'good' charged tracks
P_T Sum Density	Scalar P_T Sum of charged particles per unit $\eta - \phi$	Scalar P_T Sum of 'good' charged tracks per unit $\eta - \phi$
P_{TMax}	Maximum P_T of charged particle	Maximum P_T of 'good' charged tracks

4 Results

4.1 Correcting Back to Particle Level

We use the ratio of the generator level Monte Carlo result and the detector Level Monte Carlo result as our correction factor for correcting the data back to the particle level, as that is the effect of the detector. Our generator level results are formed by adding both electron and muon results together, since in theory level, they are expected to and indeed come out exactly similar. We put in the same kinematic cuts on both the particle level Monte Carlo and the detector level Monte carlo and data - we require that,

- Individual lepton $P_T > 20 GeV/c$,
- Individual lepton $|\eta| < 1$, and
- Lepton pair $|\eta| < 6$.

We would not show all the correction factors here, but would elucidate out method by showing one examples.

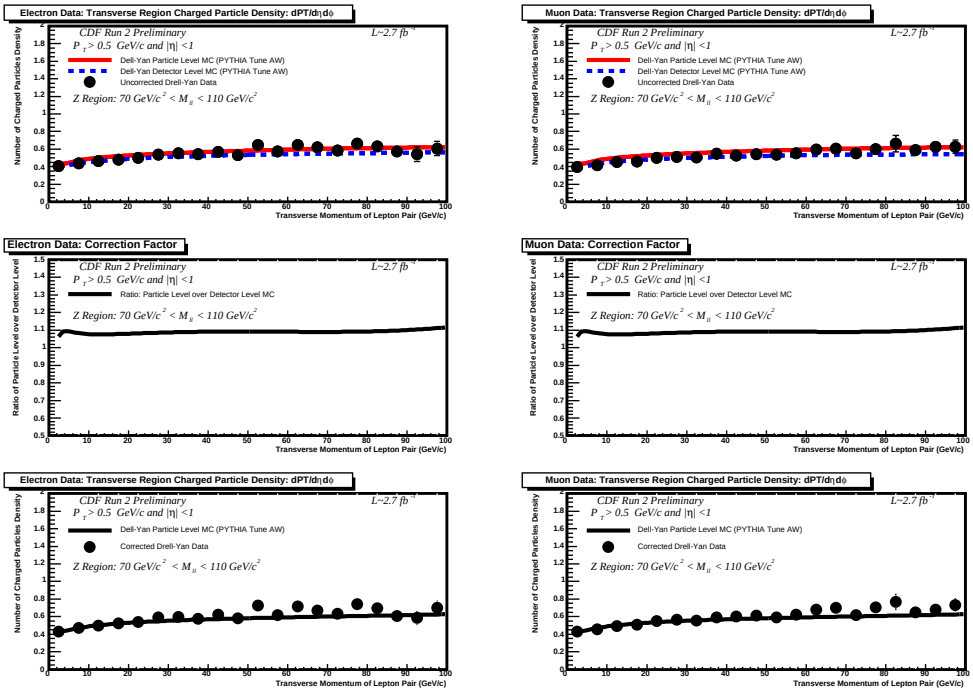

Figure 7: Step by step description of how the data are corrected back to particle level, for transverse region charged particle density, as an example. The first row shows uncorrected data, detector level Monte Carlo and particle level Monte Carlo. The second row shows the correction factor obtained by dividing the particle level Monte Carlo by detector level Monte Carlo. The third row shows the data corrected back to particle level by multiplying the correction factor obtained in the previous step. The left side is for electron data and right side is for muon data.

4.2 Systematic Uncertainties

We correct the data back to particle level in three different ways for electron, and in two different ways for muon, as shown in Table 7. We use the differences at particle level between loose-tight and tight-tight electron selection and loose and tight track cuts for charged particles as sysmatic uncertainty for electron data. For muon data, the difference between loose and tight track cuts acts as systematic error. We add the different systematic errors in quadrature, and finally add the statistical error with that in quadrature with that to draw one combined error bar. Here we show the transverse charged multiplicity plots for both electron and muon events with uncorrected data for all the different lepton and track selections, and compare that with corrected version of the same data.

We can clearly see that the differences between different cuts do not produce a significant systematic error and the dominant contribution to our total errors are statistical. When combining the results from electron and muon data, their difference acts as another source of systematic error and added in quadrature - occasionally we have large systematic error coming because of the differences in those two results. When comparing with the dijet 'underlying event' data later, we would see that they have much smaller statistical (hence overall) errors, as there are much more dijet events than Z-boson events.

Table 7: Systematic Uncertainties

Electron Data	Muon Data
Bin by bin difference between the corrected data for tight-loose electron pair with tight track cut and the corrected data for tight-loose electron pair with loose track cut	Bin by bin difference between the corrected data with tight track cut and the corrected data with loose track cut
Bin by bin difference between the corrected data for tight-loose electron pair with tight track cut and the corrected data with tight-tight electron pair and tight track cut	
Bin by bin difference between corrected electron and muon data	

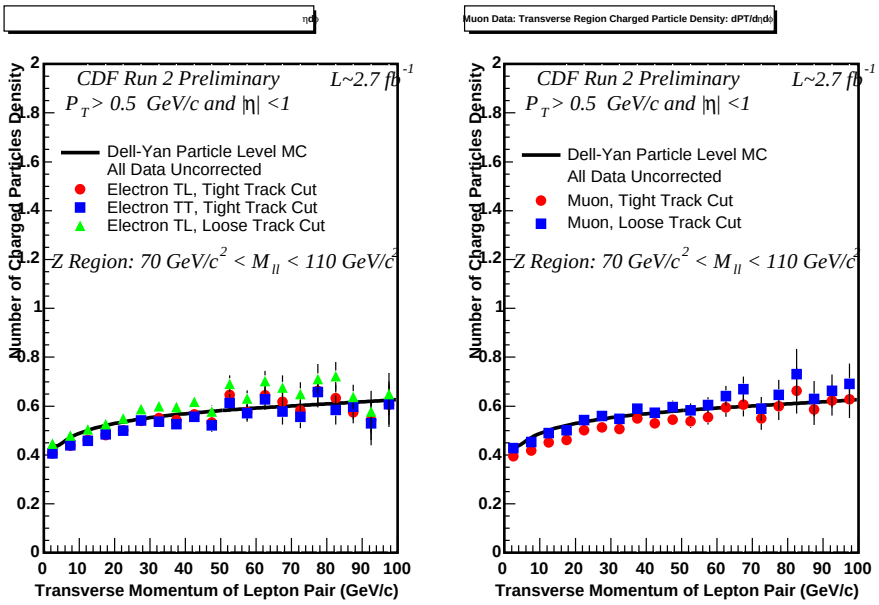

Figure 8: Shows the origin of systematic uncertainties in uncorrected data, for transverse region charged particle density, as an example. The left side is for electron data and right side is for muon data.

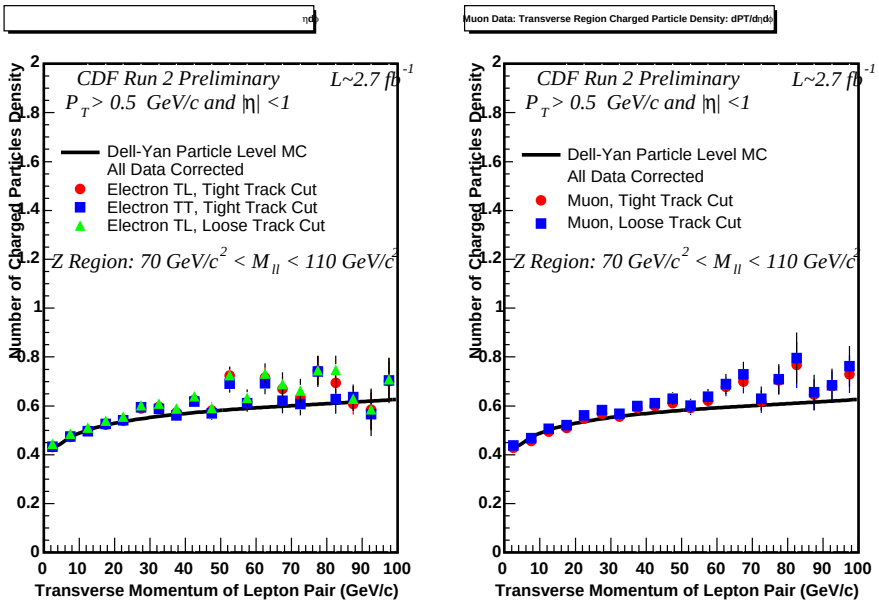

Figure 9: Shows the origin of systematic uncertainties in corrected data, for transverse region charged particle density, as an example. The left side is for electron data and right side is for muon data.

4.3 Z Region Results

We take 70 GeV/c < invariant mass of the lepton pair < 110 GeV/c as the region of the Z boson and look at the underlying event observables with respect to transverse momentum of the lepton pair. All the charged particles have $P_T > 0.5$ GeV/c and $|\eta| < 1$. We cut off at $P_T = 100$ GeV/c, above which we do not have enough statistics.

We also overlay transverse and toward regions for each observable in the same plot for comparison purpose, and then overlay the away region with them too.

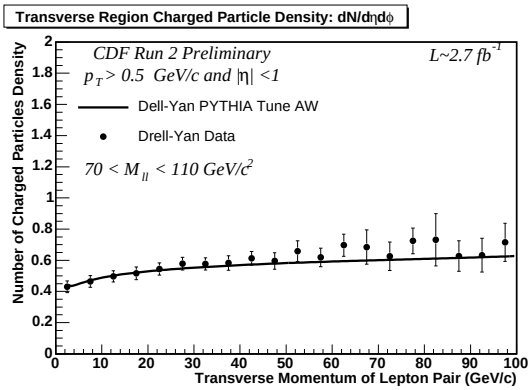

Figure 10: Transverse Region Charged Multiplicity Density, Data Corrected, Electron and Muon Data Combined ($P_T > 0.5$ GeV/c and $|\eta| < 1$). Solid line represents PYTHIA Tune AW predictions and the data are corrected back to particle level (with errors that include both the statistical error and the systematic uncertainty).

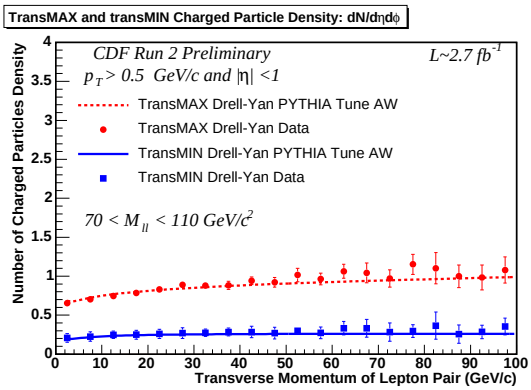

Figure 11: TransMAX and MIN Region Charged Multiplicity Density, Data Corrected, Electron and Muon Data Combined ($P_T > 0.5$ GeV/c and $|\eta| < 1$). Lines represent PYTHIA Tune AW predictions and the data are corrected back to particle level (with errors that include both the statistical error and the systematic uncertainty).

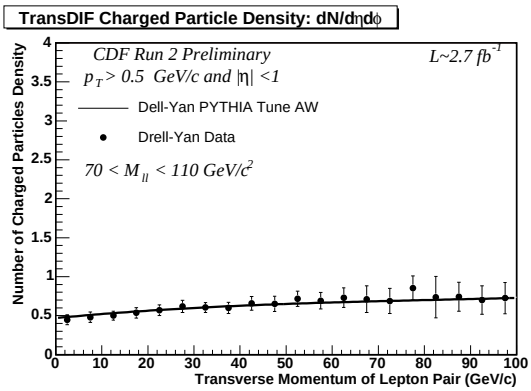

Figure 12: TransDIF Region Charged Multiplicity Density, Data Corrected, Electron and Muon Data Combined ($P_T > 0.5$ GeV/c and $|\eta| < 1$). Solid line represents PYTHIA Tune AW predictions and the data are corrected back to particle level (with errors that include both the statistical error and the systematic uncertainty).

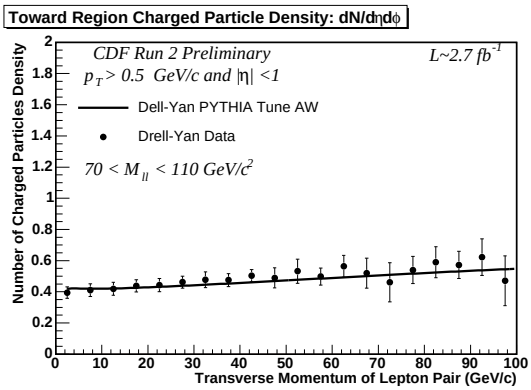

Figure 13: Toward Region Charged Multiplicity Density, Data Corrected, Electron and Muon Data Combined ($P_T > 0.5$ GeV/c and $|\eta| < 1$). Solid line represents PYTHIA Tune AW predictions and the data are corrected back to particle level (with errors that include both the statistical error and the systematic uncertainty).

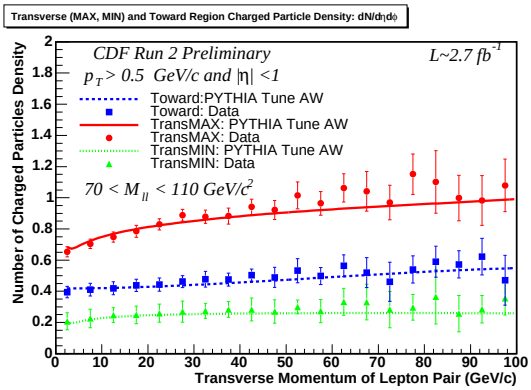

Figure 14: Transverse and Toward Region Charged Multiplicity Density, Data Corrected, Electron and Muon Data Combined ($P_T > 0.5$ GeV/c and $|\eta| < 1$). Lines represent PYTHIA Tune AW predictions and the data are corrected back to particle level (with errors that include both the statistical error and the systematic uncertainty).

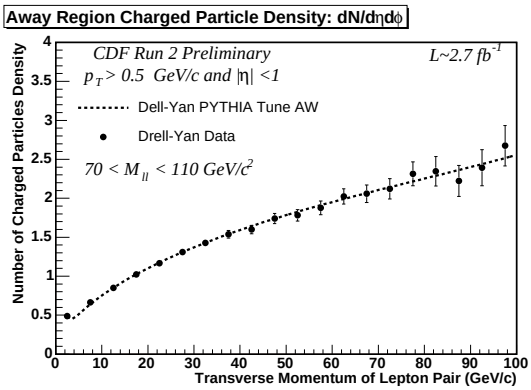

Figure 15: Away Region Charged Multiplicity Density, Data Corrected, Electron and Muon Data Combined ($P_T > 0.5$ GeV/c and $|\eta| < 1$). Solid line represents PYTHIA Tune AW predictions and the data are corrected back to particle level (with errors that include both the statistical error and the systematic uncertainty).

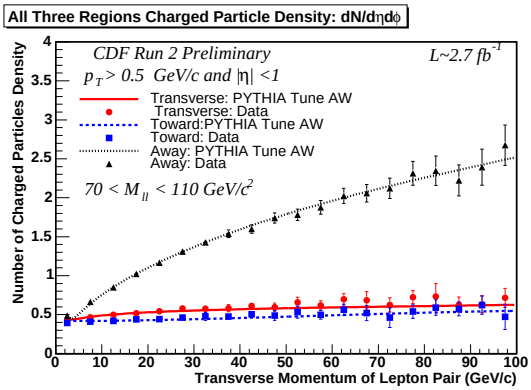

Figure 16: All Three Regions Charged Multiplicity Density, Data Corrected, Electron and Muon Data Combined ($P_T > 0.5$ GeV/c and $|\eta| < 1$). Lines represent PYTHIA Tune AW predictions and the data are corrected back to particle level (with errors that include both the statistical error and the systematic uncertainty).

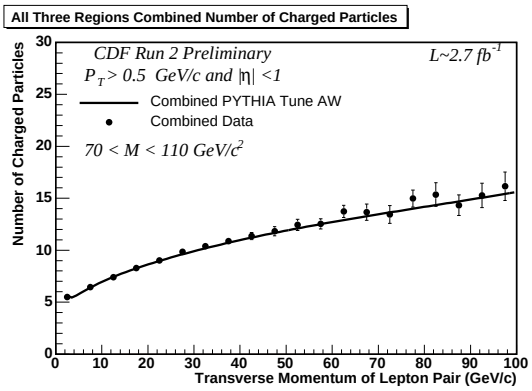

Figure 17: All Three Regions Charged Multiplicity Density Added, Data Corrected, Electron and Muon Data Combined ($P_T > 0.5$ GeV/c and $|\eta| < 1$). Solid line represents PYTHIA Tune AW predictions and the data are corrected back to particle level (with errors that include both the statistical error and the systematic uncertainty).

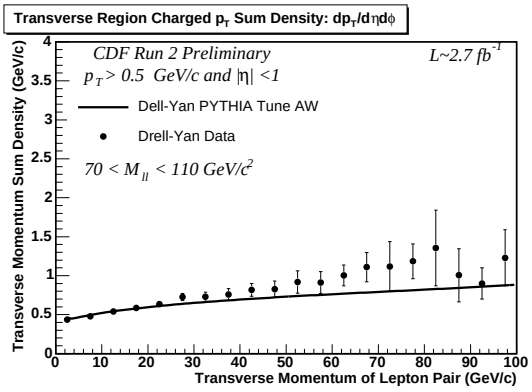

Figure 18: Transverse Region Charged P_T Sum Density, Data Corrected, Electron and Muon Data Combined ($P_T > 0.5$ GeV/c and $|\eta| < 1$). Solid line represents PYTHIA Tune AW predictions and the data are corrected back to particle level (with errors that include both the statistical error and the systematic uncertainty).

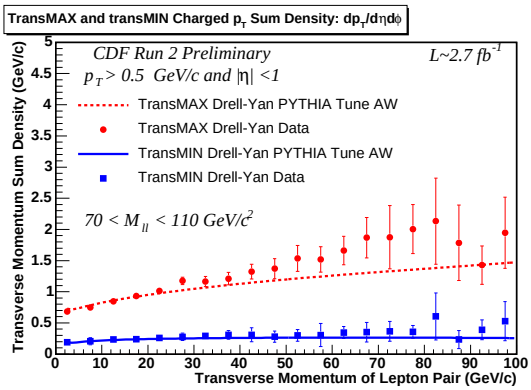

Figure 19: TransMAX and MIN Region Charged P_T Sum Density, Data Corrected, Electron and Muon Data Combined ($P_T > 0.5$ GeV/c and $|\eta| < 1$). Lines represent PYTHIA Tune AW predictions and the data are corrected back to particle level (with errors that include both the statistical error and the systematic uncertainty).

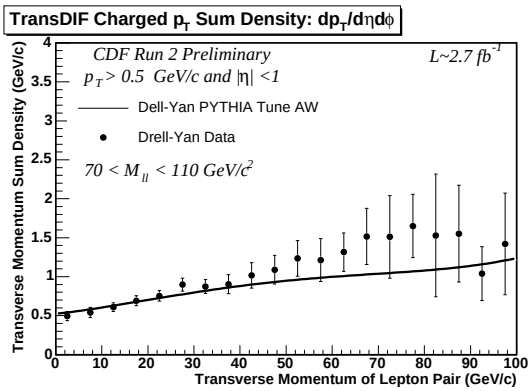

Figure 20: TransDIF Region Charged P_T Sum Density, Data Corrected, Electron and Muon Data Combined ($P_T > 0.5$ GeV/c and $|\eta| < 1$). Solid line represents PYTHIA Tune AW predictions and the data are corrected back to particle level (with errors that include both the statistical error and the systematic uncertainty).

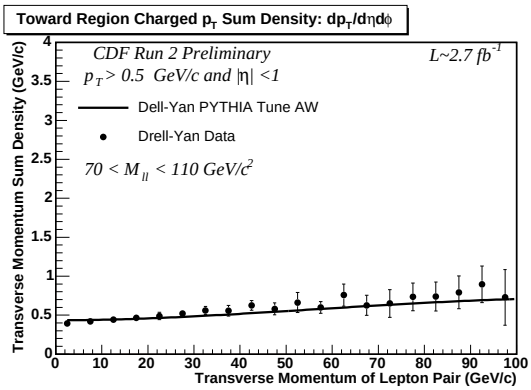

Figure 21: Toward Region Charged P_T Sum Density, Data Corrected, Electron and Muon Data Combined ($P_T > 0.5$ GeV/c and $|\eta| < 1$). Solid line represents PYTHIA Tune AW predictions and the data are corrected back to particle level (with errors that include both the statistical error and the systematic uncertainty).

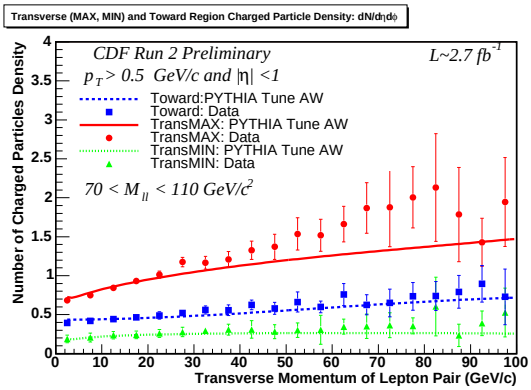

Figure 22: Transverse and Toward Region Charged P_T Sum Density, Data Corrected, Electron and Muon Data Combined ($P_T > 0.5$ GeV/c and $|\eta| < 1$). Lines represent PYTHIA Tune AW predictions and the data are corrected back to particle level (with errors that include both the statistical error and the systematic uncertainty).

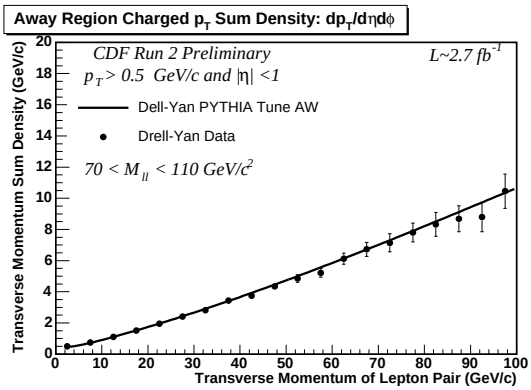

Figure 23: Away Region Charged P_T Sum Density, Data Corrected, Electron and Muon Data Combined ($P_T > 0.5$ GeV/c and $|\eta| < 1$). Solid line represents PYTHIA Tune AW predictions and the data are corrected back to particle level (with errors that include both the statistical error and the systematic uncertainty).

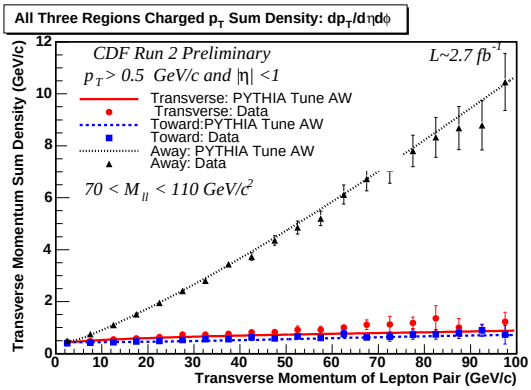

Figure 24: All Three Regions Charged P_T Sum Density, Data Corrected, Electron and Muon Data Combined ($P_T > 0.5$ GeV/c and $|\eta| < 1$). Lines represent PYTHIA Tune AW predictions and the data are corrected back to particle level (with errors that include both the statistical error and the systematic uncertainty).

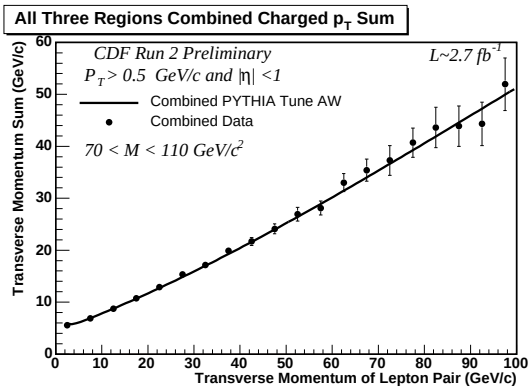

Figure 25: All Three Regions Charged P_T Sum Density Added, Data Corrected, Electron and Muon Data Combined ($P_T > 0.5$ GeV/c and $|\eta| < 1$). Solid line represents PYTHIA Tune AW predictions and the data are corrected back to particle level (with errors that include both the statistical error and the systematic uncertainty).

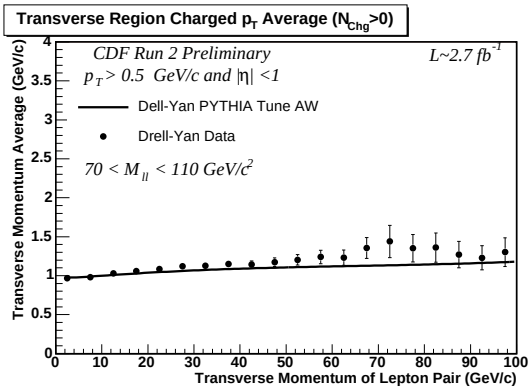

Figure 26: Transverse Region Charged P_T Average, Data Corrected, Electron and Muon Data Combined ($P_T > 0.5$ GeV/c and $|\eta| < 1$). Solid line represents PYTHIA Tune AW predictions and the data are corrected back to particle level (with errors that include both the statistical error and the systematic uncertainty).

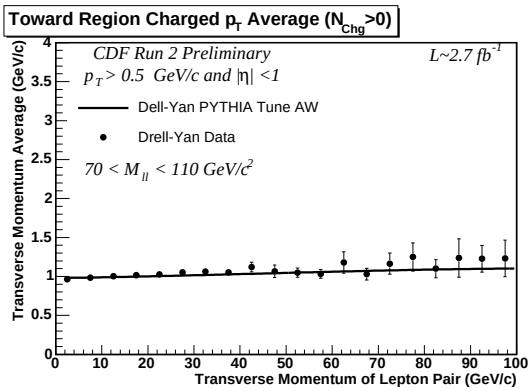

Figure 27: Toward Region Charged P_T Average, Data Corrected, Electron and Muon Data Combined ($P_T > 0.5$ GeV/c and $|\eta| < 1$). Solid line represents PYTHIA Tune AW predictions and the data are corrected back to particle level (with errors that include both the statistical error and the systematic uncertainty).

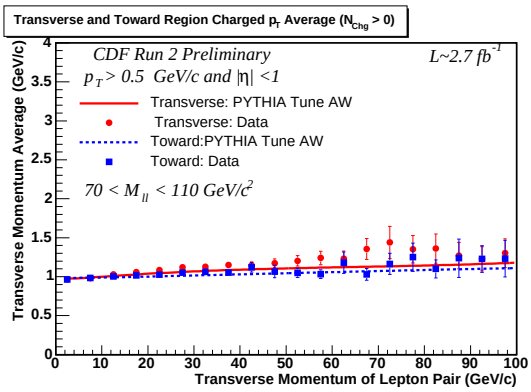

Figure 28: Transverse and Toward Region Charged P_T Average, Data Corrected, Electron and Muon Data Combined ($P_T > 0.5$ GeV/c and $|\eta| < 1$). Lines represent PYTHIA Tune AW predictions and the data are corrected back to particle level (with errors that include both the statistical error and the systematic uncertainty).

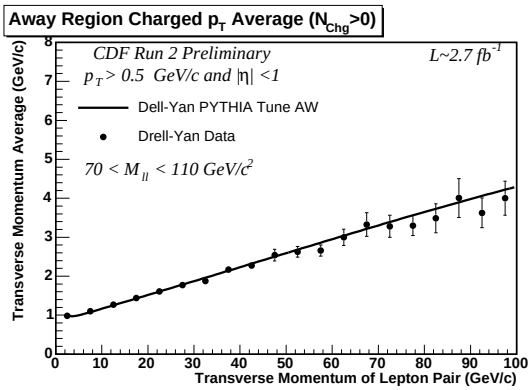

Figure 29: Away Region Charged P_T Average, Data Corrected, Electron and Muon Data Combined ($P_T > 0.5$ GeV/c and $|\eta| < 1$). Solid line represents PYTHIA Tune AW predictions and the data are corrected back to particle level (with errors that include both the statistical error and the systematic uncertainty).

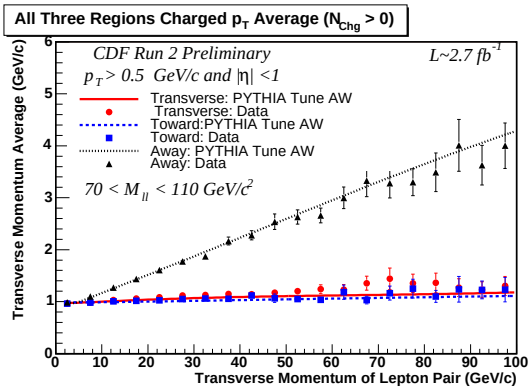

Figure 30: All Three Regions Charged P_T Average, Data Corrected, Electron and Muon Data Combined ($P_T > 0.5$ GeV/c and $|\eta| < 1$). Lines represent PYTHIA Tune AW predictions and the data are corrected back to particle level (with errors that include both the statistical error and the systematic uncertainty).

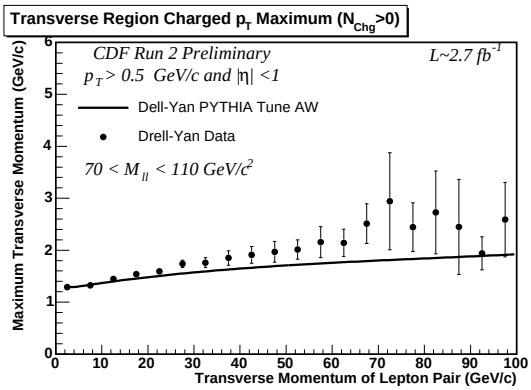

Figure 31: Transverse Region Charged P_T Maximum, Data Corrected, Electron and Muon Data Combined ($P_T > 0.5$ GeV/c and $|\eta| < 1$). Solid line represents PYTHIA Tune AW predictions and the data are corrected back to particle level (with errors that include both the statistical error and the systematic uncertainty).

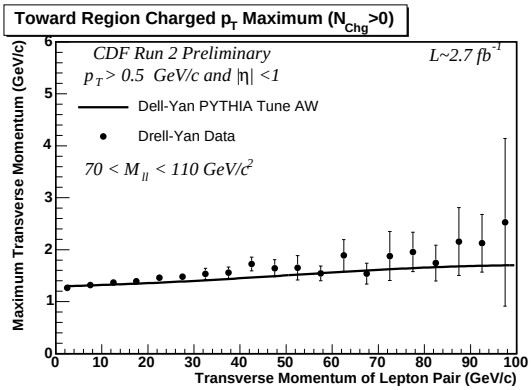

Figure 32: Toward Region Charged P_T Maximum, Data Corrected, Electron and Muon Data Combined ($P_T > 0.5$ GeV/c and $|\eta| < 1$). Solid line represents PYTHIA Tune AW predictions and the data are corrected back to particle level (with errors that include both the statistical error and the systematic uncertainty).

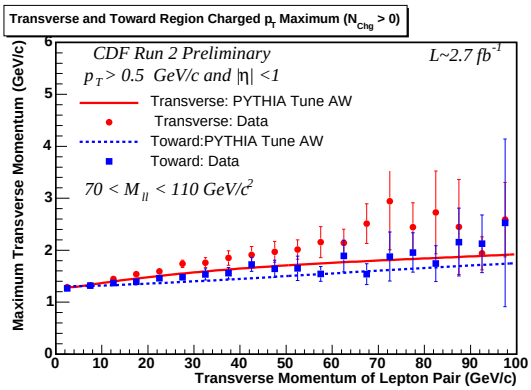

Figure 33: Transverse and Toward Region Charged P_T Maximum, Data Corrected, Electron and Muon Data Combined ($P_T > 0.5$ GeV/c and $|\eta| < 1$). Lines represent PYTHIA Tune AW predictions and the data are corrected back to particle level (with errors that include both the statistical error and the systematic uncertainty).

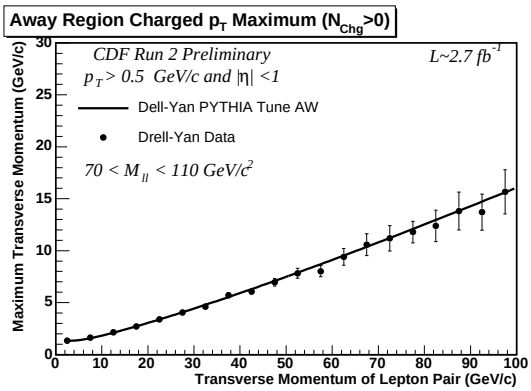

Figure 34: Away Region Charged P_T Maximum, Data Corrected, Electron and Muon Data Combined ($P_T > 0.5$ GeV/c and $|\eta| < 1$). Solid line represents PYTHIA Tune AW predictions and the data are corrected back to particle level (with errors that include both the statistical error and the systematic uncertainty).

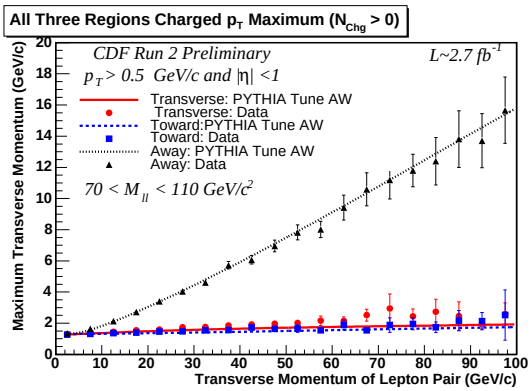

Figure 35: All Three Regions Charged P_T Maximum, Data Corrected, Electron and Muon Data Combined ($P_T > 0.5$ GeV/c and $|\eta| < 1$). Lines represent PYTHIA Tune AW predictions and the data are corrected back to particle level (with errors that include both the statistical error and the systematic uncertainty).

4.4 Compared with Leading Jet Underlying Event

Here we compare our results with leading jet underlying events results from [2]. Mostly we observe a very good match, as expected. We have to note that dijet and Drell-Yan events have distinct topologies. At very low P_T, Z-boson still has the large invariant mass, whereas we only get minbias events for dijet in that region - which explains the apparent mismatch between dijet and Drell-Yan 'underlying events' in low P_T region.

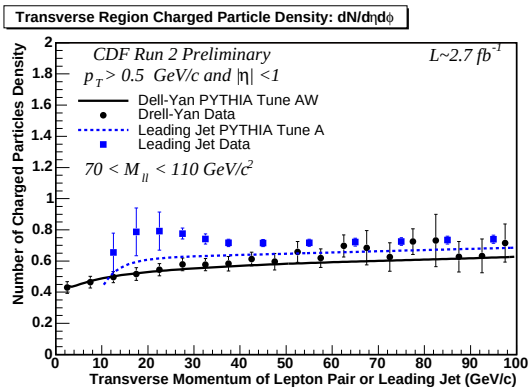

Figure 36: Transverse Region Charged Multiplicity Density, Data Corrected, Electron and Muon results combined, compared with Leading Jet result ($P_T > 0.5$ GeV/c and $|\eta| < 1$). Lines represent PYTHIA predictions and the data are corrected back to particle level (with errors that include both the statistical error and the systematic uncertainty).

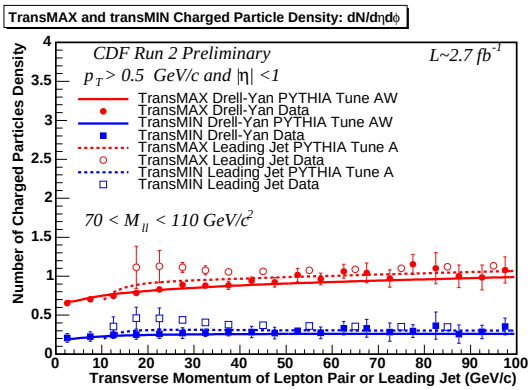

Figure 37: TransMAX and MIN Region Charged Multiplicity Density, Data Corrected, Electron and Muon results combined, compared with Leading Jet result ($P_T > 0.5$ GeV/c and $|\eta| < 1$) . Lines represent PYTHIA predictions and the data are corrected back to particle level (with errors that include both the statistical error and the systematic uncertainty).

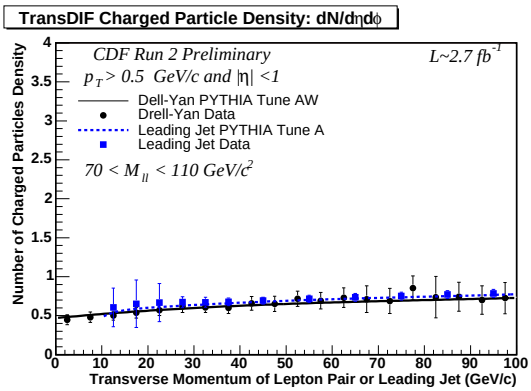

Figure 38: TransDIF Region Charged Multiplicity Density, Data Corrected, Electron and Muon results combined, compared with Leading Jet result ($P_T > 0.5$ GeV/c and $|\eta| < 1$). Lines represent PYTHIA predictions and the data are corrected back to particle level (with errors that include both the statistical error and the systematic uncertainty).

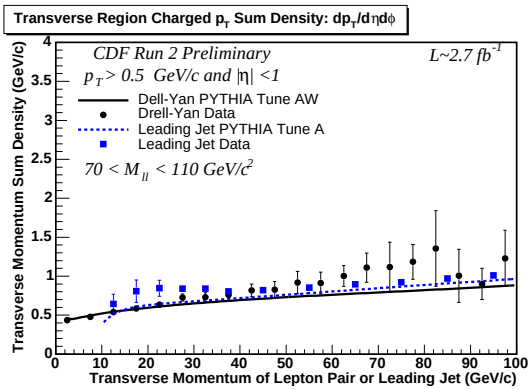

Figure 39: Transverse Region Charged P_T Sum Density, Data Corrected, Electron and Muon results combined, compared with Leading Jet result ($P_T > 0.5$ GeV/c and $|\eta| < 1$). Lines represent PYTHIA predictions and the data are corrected back to particle level (with errors that include both the statistical error and the systematic uncertainty).

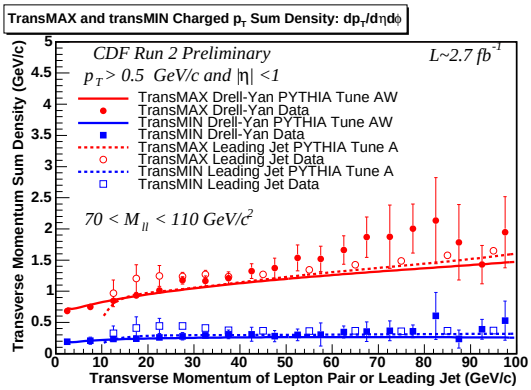

Figure 40: TransMAX and MIN Region Charged P_T Sum Density, Data Corrected, Electron and Muon results combined, compared with Leading Jet result ($P_T > 0.5$ GeV/c and $|\eta| < 1$). Lines represent PYTHIA predictions and the data are corrected back to particle level (with errors that include both the statistical error and the systematic uncertainty).

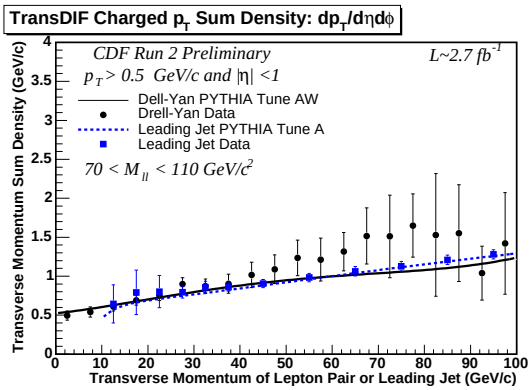

Figure 41: TransDIF Region Charged P_T Sum Density, Data Corrected, Electron and Muon results combined, compared with Leading Jet result ($P_T > 0.5$ GeV/c and $|\eta| < 1$). Lines represent PYTHIA predictions and the data are corrected back to particle level (with errors that include both the statistical error and the systematic uncertainty).

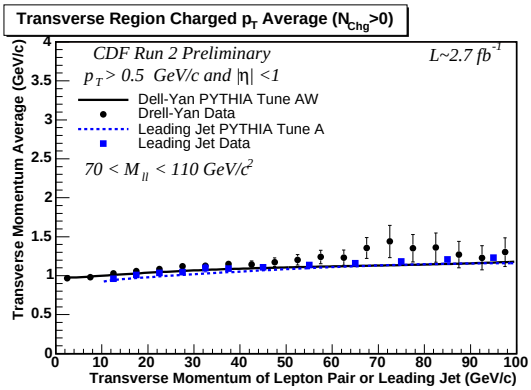

Figure 42: Transverse Region Charged P_T Average, Data Corrected, Electron and Muon results combined, compared with Leading Jet result ($P_T > 0.5$ GeV/c and $|\eta| < 1$). Lines represent PYTHIA predictions and the data are corrected back to particle level (with errors that include both the statistical error and the systematic uncertainty).

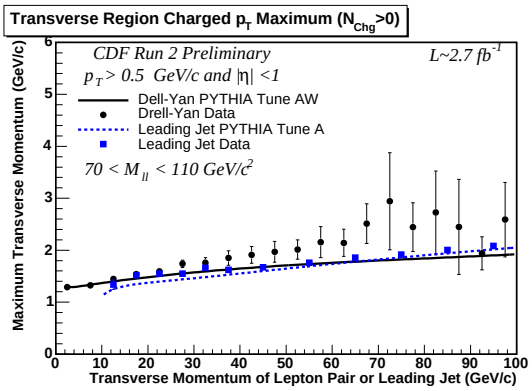

Figure 43: Transverse Region Charged P_T Maximum, Data Corrected, Electron and Muon results combined, compared with Leading Jet result ($P_T > 0.5$ GeV/c and $|\eta| < 1$). Lines represent PYTHIA predictions and the data are corrected back to particle level (with errors that include both the statistical error and the systematic uncertainty).

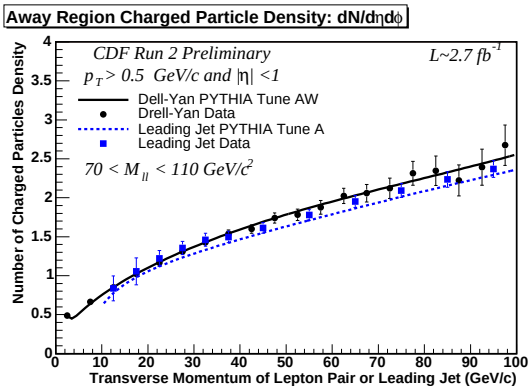

Figure 44: Away Region Charged Multiplicity Density, Data Corrected, Electron and Muon results combined, compared with Leading Jet result ($P_T > 0.5$ GeV/c and $|\eta| < 1$). Lines represent PYTHIA predictions and the data are corrected back to particle level (with errors that include both the statistical error and the systematic uncertainty).

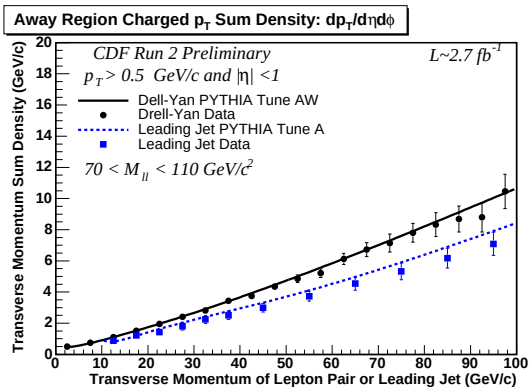

Figure 45: Away Region Charged P_T Sum Density, Data Corrected, Electron and Muon results combined, compared with Leading Jet result ($P_T > 0.5$ GeV/c and $|\eta| < 1$). Lines represent PYTHIA predictions and the data are corrected back to particle level (with errors that include both the statistical error and the systematic uncertainty).

4.5 Correlation Plots

The correlation between mean P_T and charged multiplicity is useful to look at the interplay between different mechanisms for underlying events. First we would show how the plots are arrived at, followed by the plots themselves.

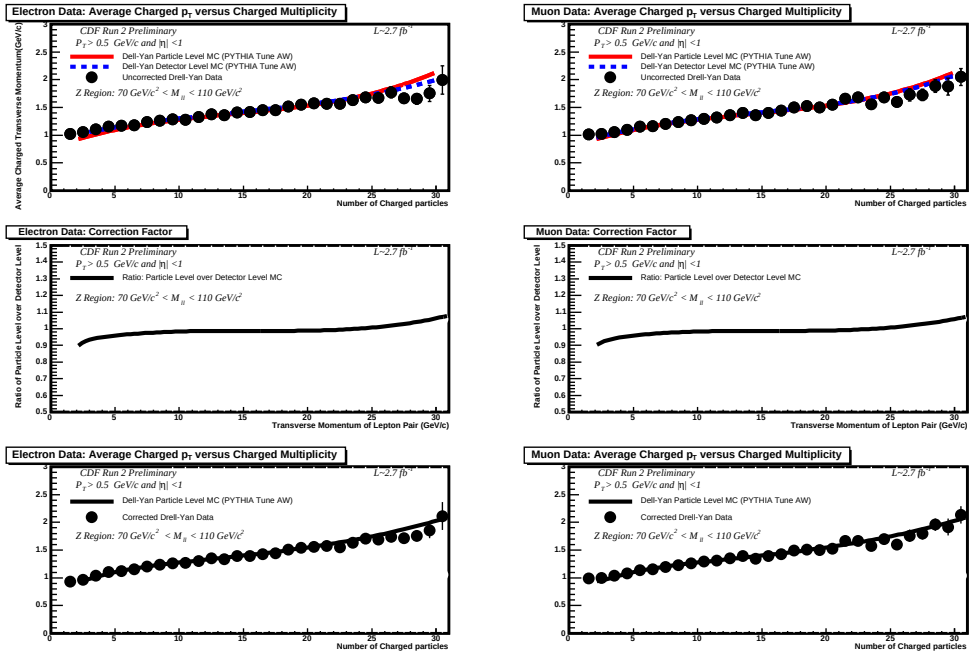

Figure 46: Step by step description of how the data are corrected back to particle level, for charged P_T average versus charged multiplicity. The first row shows uncorrected data, detector level Monte Carlo and particle level Monte Carlo. The second row shows the correction factor obtained by dividing the particle level Monte Carlo by detector level Monte Carlo. The third row shows the data corrected back to particle level by multiplying the correction factor obtained in the previous step. The left side is for electron data and right side is for muon data.

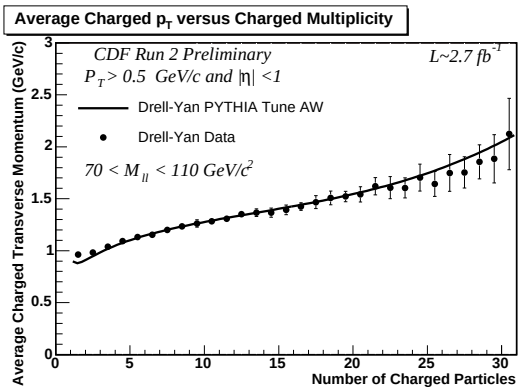

Figure 47: Drell-Yan charged p_T average and charged multiplicity correlation, electron and muon data combined ($p_T > 0.5$ GeV/c and $|\eta| < 1$). Solid line represents PYTHIA Tune AW predictions and the data are corrected back to particle level (with errors that include both the statistical error and the systematic uncertainty).

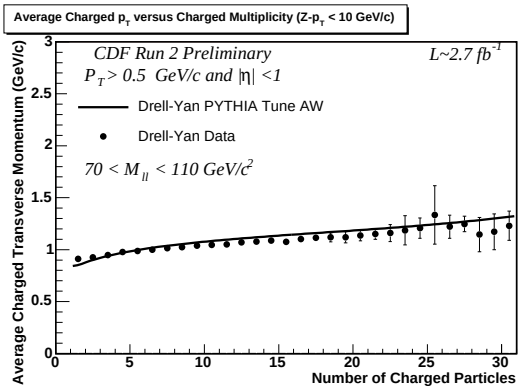

Figure 48: Drell-Yan charged p_T average and charged multiplicity correlation, with Z-p_T < 10 GeV/c, electron and muon data combined ($p_T > 0.5$ GeV/c and $|\eta| < 1$). Solid line represents PYTHIA Tune AW predictions and the data are corrected back to particle level (with errors that include both the statistical error and the systematic uncertainty).

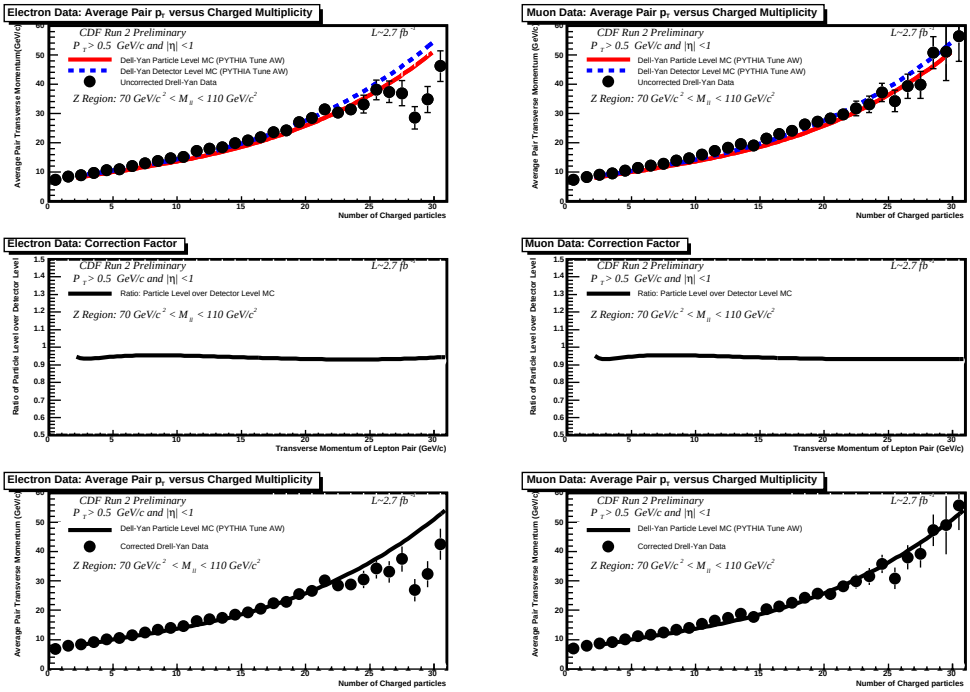

Figure 49: Step by step description of how the data are corrected back to particle level, for pair P_T average versus charged multiplicity. The first row shows uncorrected data, detector level Monte Carlo and particle level Monte Carlo. The second row shows the correction factor obtained by dividing the particle level Monte Carlo by detector level Monte Carlo. The third row shows the data corrected back to particle level by multiplying the correction factor obtained in the previous step. The left side is for electron data and right side is for muon data.

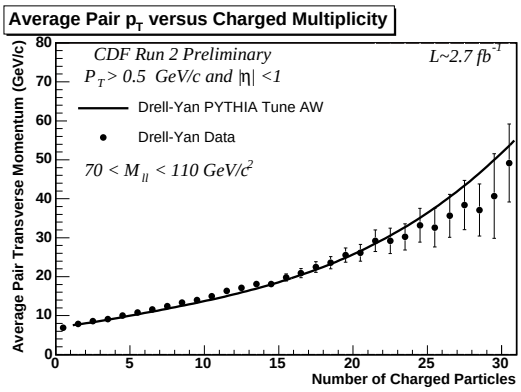

Figure 50: Drell-Yan pair p_T average and charged multiplicity correlation, electron and muon data combined ($p_T > 0.5$ GeV/c and $|\eta| < 1$). Solid line represents PYTHIA Tune AW predictions and the data are corrected back to particle level (with errors that include both the statistical error and the systematic uncertainty).

4.6 Summary

We studied the underlying event variables associated with Drell Yan lepton pair production and mostly observed excellent agreements with PYTHIA Tune AW Monte Carlo predictions. We also compared them with leading jet underlying event results and observed a reasonably close match - which may indicate the universality of underlying event modeling. For charged particle density and charged particle transverse momentum sum, we observe a slight excess at transverse region compared to toward region, which is caused by transverse regions receiving contributions from away side jet.

References

[1] Richard D.Field, *Applications of Perturbative QCD*

Addison-Wesley Publishing Company, 1989.

[2] Rick Field and Craig Group

CDF-QCD Data for Theorists (Part 1) Leading Jet events

CDF Note - CDF/ANAL/CDF/CDFR/9087

[3] Alberto Cruz, Rick Field and Craig Group

Using MAX/MIN Transverse Regions to Study the Underlying Event in Run 2 at the Tevatron

CDF Note - CDF/ANAL/CDF/CDFR/7703

[4] T. Spreitzer, C. Mills and J. Incandela

Electron Identification in Offline Release 6.1.2

CDF Note - CDF/DOC/ELECTRON/CDFR/7950

[5] Ulysses Grundler, Anyes Taffard and Xiaojian Zhang

High-P_T muons recommended cuts and efficiencies for Summer 2006

CDF Note - CDF/ANAL/TOP/CDFR/8262

[6] Tracey Pratt, Koji Ikado, Kaori Maeshima and Todd Huffman

Resonance Searches in high mass dimuons

CDF Note - CDF/ANAL/EXOTIC/CDFR/6073

[7] Young-kee Kim and Un-ki Yang

Initial state gluon radiation studies on Drell-Yan data for top-pair production in

hadron collider

CDF Note - CDF/PHYS/TOP/CDFR/6804

[8] Richard D.Field, Research Webpage

http://www.phys.ufl.edu/$\sim rfield/RDF\_res.html$

[9] Drell Yan figures

http://www.rarf.riken.go.jp/rarf/rhic/phys/DY/DY.html